

## **Schlieren and Shadowgraph Imaging in the Great Outdoors**

**Gary S. Settles**

*Gas Dynamics Lab, Mechanical & Nuclear Engineering Dept., Penn State University*  
*301D Reber Bldg., University Park, PA 16802 USA*

*E-mail: [gss2@psu.edu](mailto:gss2@psu.edu) URL: <http://www.me.psu.edu/psgdl>*

A review is given of outdoor schlieren and shadowgraph imaging, beginning with an historical perspective. The optical principles of the sunlight shadowgraph method and schlieren observation by background distortion are discussed. Examples and illustrations are given of the visualization of outdoor thermal convection, combustion, and explosion phenomena. Jet aircraft and high-speed flight are featured as important subjects for such flow visualization. Finally, though most of these examples are visible to the unaided eye, some instruments are available for enhanced outdoor refractive imaging in special cases.

### **INTRODUCTION**

The shadowgraph and schlieren methods are generally regarded as items of laboratory apparatus for visualizing inhomogeneities in transparent media. While shadows are routinely cast outdoors by the sun, it is well known that schlieren imaging requires a lens and, in particular, a cutoff of refracted light rays. Since the transparent medium under study must be interposed between these optical elements and a suitable light source, it seems at first unlikely that such an optical arrangement would occur naturally. Nonetheless it does occur, and one may often see examples of shadowgrams and schlieren images in the great outdoors if one knows where and how to look for them.

The father of the optics of inhomogeneous media, Robert Hooke (1635-1703), first discussed these natural visualizations in Observation LVIII of his famous *Micrographia*[1]. Having covered light refraction due to density variations in the atmosphere and in liquids, Hooke proceeded to explain the twinkling of stars, “heat haze,” mirages, and the distortion of the setting sun seen through a chimney plume. He understood these optical phenomena thoroughly, and was able to generalize laboratory instruments from such outdoor observations. Unfortunately his invention of the schlieren technique – demonstrated before the Royal Society in 1672 – was far ahead of its time[2] and was never put to significant use by Hooke or by his peers.

Two centuries later, Ernst Mach mentioned several outdoor shadowgraph and schlieren visualizations in his *Popular Scientific Lectures*[3]. These included background distortion due to convection from objects heated by the sun, and sunlight shadowgraphy of the blast wave from a dynamite explosion (the latter related to Mach by C. V. Boys). He further tells the story of the French artilleryman Journée, who claimed to have seen by eye certain waves trailing from a high-speed projectile that he followed telescopically. This, plus the questionable gas-dynamic speculations of Belgian ballistician Melsens[4] and the then-unproved shock wave theory of Riemann[5] may have urged Mach onward to take, in 1887, the world’s first photos of shock waves from bullets in flight[6].

At the beginning of the 20<sup>th</sup> Century, American astronomer A. E. Douglass turned his attention from the stars to the annoying atmospheric disturbances[7] which interfered with his telescopic “seeing”. His sketches and descriptions of atmospheric turbulence, as observed directly through the telescope by starlight shadowgraphy, foreshadowed the modern field of atmospheric optical propagation.

Hubert Schardin, the modern patriarch of optical flow visualization, began his 1942 treatise on

schlieren techniques and their applications[8, 9] by remarking upon schlieren that are visible to the naked eye in windowpanes and above hot railroad tracks. This served to introduce a thorough review of a dozen different laboratory instruments for schlieren and shadowgraphy, along with their many diverse applications.

Finally, Cooper and Rathert[10] first studied the use of sunlight shadowgraphy to reveal shock wave locations on high-speed aircraft wings. Their work was done in 1948, a year after the “sound barrier” was first officially broken by an airplane. The complexity of transonic flow was both mysterious and dangerous then, and tools to study it were scarce. To some extent this still holds true.

Such historical and anecdotal examples of outdoor schlieren and shadowgraphy have been known, more or less, for many years, but the topic has yet to be treated as a coherent whole. There is potential value here, not only in a better understanding of natural phenomena through flow visualization, but also in the possibility that new techniques and visualizations may arise from such considerations. A general review of outdoor schlieren and shadowgraphy is thus the purpose of the present paper.

## OPTICAL PRINCIPLES

### Sunlight Shadowgraphy

The circumstances under which the sun casts a shadowgram upon an available surface are diagrammed in Fig. 1. Since the sun subtends an angle of about  $1/2^\circ$  (31 minutes of arc) at our average distance from it, it immediately fails the primary criterion for good shadowgraphy: that of a “point” light source. (Sunlight shadowgrams would be sharper on the more distant planets.) Nevertheless the sun excels for this purpose in most other respects, being sufficiently intense and readily available to cast shadowgrams on an enormous scale if required.

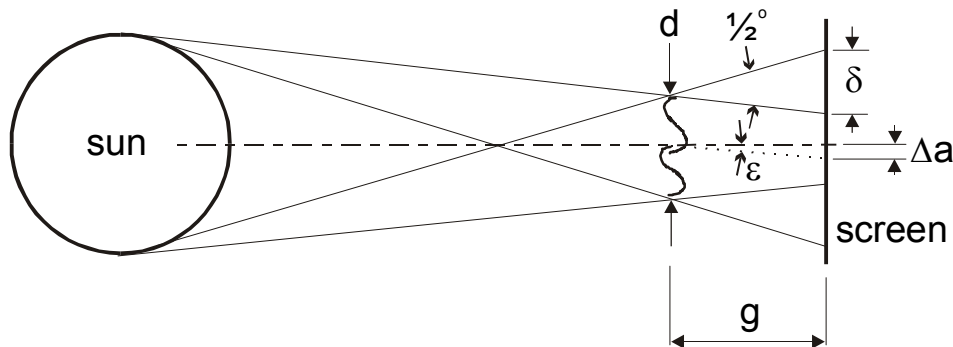


**Fig. 1** Diagram of sunlight shadowgram formation

As shown in the Figure, a “schlieren object” or refractive disturbance of lateral size  $d$  occurs at distance  $g$  from a screen upon which the shadowgram is cast. The sun’s distance is effectively infinite, but due to its apparent size the shadow of the schlieren object cannot be perfectly sharp. Rather a blurred region (penumbra) of width  $\delta$  surrounds it, where

$$\delta / g = \tan(1/2^\circ) = 0.009 \quad (1)$$

Thus the blur is linearly proportional to the object-to-screen distance  $g$ , which must be minimized if a sharp shadow is desired. (Recall here that a shadowgram is not a focused image, since no lens is involved, and thus it does not generally bear a 1:1 relationship to the schlieren object which casts it.)

The sensitivity of sunlight shadowgraphy to a ray deflected through an angle  $\epsilon$  by the schlieren object is related to the change in illumination thus caused on the screen.  $\Delta a$  denotes the ray displacement on the screen due to this deflection (Schardin[8, 9]), and is given by

$$\Delta a = g \cdot \tan \epsilon \quad (2)$$

One measure of sunlight shadowgraph sensitivity is thus to compare the magnitude of the ray deflection

with that of the blur zone:

$$\frac{\Delta a}{\delta} = \frac{\tan \varepsilon}{\tan(1/2^\circ)} \approx \frac{\varepsilon}{1/2^\circ} \quad (3)$$

From this we learn that, irrespective of standoff distance  $g$ , ray deflections by the schlieren object must compete with a substantial blur angle in order to be visible. Weak disturbances, like the thermal convection from the human body ( $\varepsilon \sim$  a few arcseconds), therefore have little chance of being seen by sunlight shadowgraphy, since the deflection-to-blur ratio of Eqn. 3 tends to zero in these cases. Strong convective plumes, defects in glass, and shock waves are another matter.

A simple experiment with a candle and a sheet of paper, in the spirit of Hooke, is further revealing: The lateral dimension  $d$  of the candle plume is on the order of 1 cm. For  $g/d \rightarrow 0$  the sunlight shadowgraph sensitivity vanishes, as expected. Unacceptable blur is observed for  $g/d$  on the order of 100 or more. The best compromise of sensitivity to blur occurs roughly when  $20 \leq g/d \leq 30$  (see Fig. 2). For the much-stronger deflections in a drinking glass or glass bottle, however, sharp sunlight shadowgrams of adequate sensitivity appear even for  $g/d$  approaching unity.

Shock waves in the air constitute another special case for sunlight shadowgraphy. As in normal shadowgraphy, nothing is seen by looking through the shock, and a shadowgram appears only when the shock and the sunlight are approximately tangent to one another. In this case the lateral extent of the shock, i.e. its thickness, is infinitesimal and the second derivative of refractive index across it – which generates the ray deflection – is quite large even for weak shocks. Thus high sensitivity is not required despite the blur encountered in sunlight. Good sunlight shadowgrams are obtained for shock waves that are very near the surfaces upon which they are cast, as is the case for airblasts originating on or near the ground, and for the transonic aircraft wing flows discussed later in this paper.



**Fig. 2** Sunlight shadowgram of the convective plume from a candle flame (photo by author)

Finally, the problem of blur in sunlight shadowgraphy can be improved by any means which limits the apparent size of the sun, as for example by the use of a lens to focus the sun's image upon a small aperture before casting the shadow. This is exactly what was done by Vincenz Dvorák, who for many years was credited with inventing shadowgraphy[11]. It was previously done by the infamous Jean-Paul Marat[12, 13], in his alter ego as a scientist, a century before Dvorák. An outdoor optical arrangement to accomplish this reduction of the sun's apparent size will be described in the final section of this paper.

### **Schardin's Schlieren Method # 1 (Background Distortion)**

The first of Schardin's several canonical schlieren arrangements[8, 9] describes the case where outdoor optical inhomogeneities become visible to the naked eye or camera through background

distortion. Striped, mottled, or checkered backgrounds can serve this purpose, but all are exemplified by the simplest case of a distant, linear light/dark boundary, as shown in Fig. 3.

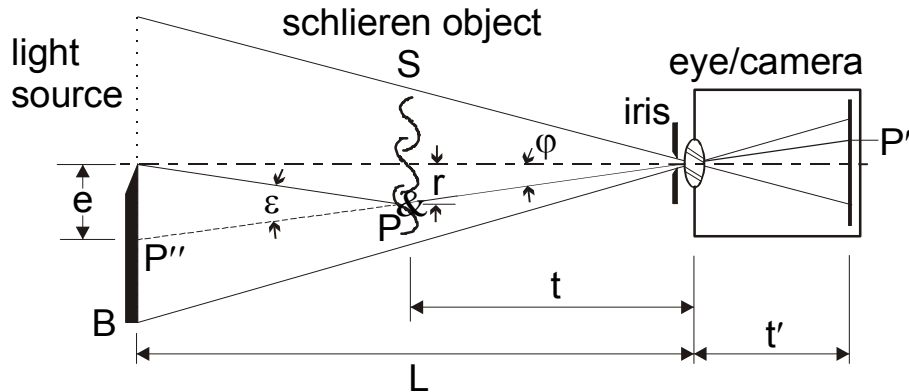


**Fig. 3** Diagram of Schardin's Schlieren Method # 1

The schlieren object  $S$  is observed by the eye or camera, which images it inverted upon the retina or film. A light/dark boundary at distance  $L$  lies on the optical axis. (Practically speaking this is often the horizon, or else the sun's disk provides the light source against the darker sky.) The image in the eye or camera portrays this inverted light/dark boundary, though it is generally defocused unless the iris is severely stopped down, or else both  $t$  and  $L$  are very large compared to  $t'$ . Point  $P$  in the schlieren object, at distance  $t$ , refracts the light from the light/dark boundary through angle  $\epsilon$ .  $P$  thus appears bright in the image at  $P'$ , even though its apparent location  $P''$  lies at an apparent distance  $e$  into the dark zone.  $P$  and  $P''$  are both characterized by viewing angle  $\phi$  below the optical axis. (In case  $t = L/2$ , then  $\phi$  and  $\epsilon$  are of equal magnitude.) The result of all this is that the distant light/dark boundary no longer appears straight in the schlieren image, but rather is distorted due to the refraction of schlieren object  $S$ . Thus the transparent refractive schlieren object, though invisible purely of itself, is rendered at least partially visible by the distortion of the background.

We have a light source, a schlieren object, and a lens producing an image of this object. It only remains to have a cutoff or knife edge, and that role is filled in Fig. 3 by the iris aperture of the camera or of the eye. This constitutes the schlieren method in its simplest generic form.

However, despite its natural occurrence without the aid of apparatus, this schlieren technique suffers the severe limitation that its working range is confined narrowly to the vicinity of the light/dark boundary. Right on this boundary the sensitivity is high, but points of the schlieren object lying off the boundary at significant viewing angles  $\phi$  must produce large ray deflections in order to become visible. Thus high sensitivity is not available over a significant field of view, and a complete impression of the schlieren image cannot be obtained without scanning. In the great outdoors, moving the eye or the camera may accomplish this while the other optical elements remain relatively fixed. In a few cases one may take advantage of the natural motion of the schlieren object for this purpose.

Almost always, in such outdoor visualizations, it is helpful to open the lens iris aperture sufficiently to defocus somewhat the distant light/dark boundary in the schlieren image. This extends the working range in the direction perpendicular to the boundary at the expense of the peak sensitivity, as in the case of increasing the light-source size in the classical Toepler schlieren system[14]. Finally, one may also move the eye or camera closer to the schlieren object  $S$ , reducing distance  $t$ , in order to slightly improve sensitivity at the expense of a narrower field-of-view of the schlieren object.

For a practical example, consider the observation of the hot-air discharge from a factory exhaust stack, seen by the naked eye against the light/dark boundary of a mountaintop. Let  $L \approx 3$  km,  $t \approx 200$  m, and the apparent radius of the background distortion in the object plane  $r \approx 1$  m (judged in comparison to the stack diameter). The viewing angle  $\phi$  of the maximum ray deflection is thus

$$\phi = \sin^{-1}(r/t) = \sin^{-1}(1/200) = 0.28^\circ \quad (4)$$

and the maximum ray deflection angle in the stack exhaust is given by

$$\varepsilon_{\max} = \tan^{-1}\left(\frac{e}{L-t}\right) = \tan^{-1}\left(\frac{L \sin \varphi}{2800}\right) = 0.3^\circ \quad (5)$$

A ray deflection of  $0.3^\circ$  is quite strong for schlieren phenomena in the atmosphere, and is not likely to persist far from the stack exit due to turbulent mixing with the atmosphere. Thus, the requirement for so strong a deflection to be visible at only 1 m displacement from the optical axis reveals the salient limitation of the background-distortion schlieren method. Despite this limitation, however, many useful visualizations can be made.

### OUTDOOR SCHLIEREN OBSERVATION BY BACKGROUND DISTORTION

The remainder of this paper consists of examples collected from various sources, and over several years of outdoor observation. Proceeding from the example just given, consider first a case often seen during freeway driving: The exhaust stacks of many large trucks discharge upward above the cab roofline. While driving on the freeway, one sees these trucks cross the horizon line ahead, whereupon the turbulent exhaust plume becomes briefly visible through background distortion.

A simple experiment was performed in which a propane torch was placed upon a porch rail and imaged, via telephoto lens, against a background of distant trees (see Fig. 4). The lighting was such that the tree limbs and leaves appeared dark against a bright sky, and provided a random light/dark background rather than a horizontal line. Videotape was shot over the range of available camera lens apertures, with the focus always sharply upon the torch. Stopped-down cases where both the trees and the torch were in focus did not yield very effective visualizations of the torch plume. However, upon opening the iris, a point was reached where the plume stood out starkly against the blurred, mottled light/dark background. This background distortion effect of a multiplicity of light/dark edges then merged into a single visualization of a foreground schlieren object in focus against an unsharp background. Motion cues played an important role, so the image in Fig. 4 is not truly representative. Nevertheless this appears to be partly a mental phenomenon: beyond a certain background blur level, the brain ignores the background and concentrates on the sharp foreground, yielding a pseudo-three-dimensional effect. One might call it “psychological schlieren imaging.”



**Fig. 4** Video frame of propane torch seen against distant trees (image by author)

Everyone sees, and routinely ignores, the background distortion effect caused by convection about hot objects in the sun. This is seldom clearer than the case of a hot car roof observed against a suitable background. The thermal boundary layer on the roof, apparently one or two cm thick, is hard to miss.

Fig. 5 shows such a case, where the ventilation gratings of a nearby building provided an ideal background. Several photos were taken with an ordinary 35mm camera while progressively reducing the lens aperture. The best result – shown in the figure – is the case of the largest aperture at which the background gridlines are resolved sufficiently to be seen with good contrast. The reverse curvature of these gridlines in the car roof boundary layer is the result of the light being refracted with a component to the left, in which direction the air density increases in this particular example.



**Fig. 5** Thermal boundary layer on hot car roof, seen by distortion of background grid pattern (photo by author).

Some experiments can only be performed outdoors, where conventional optical apparatus is unavailable. This is the case with large explosions, which must then depend upon background distortion to reveal shock wave motion, etc. Fig. 6 is an outstanding example. Following the above-ground nuclear test ban treaty some decades ago, it still remains possible to approximate nuclear blast effects by setting off very large conventional chemical explosions. The scale of the one shown in Fig. 6 is indicated by the trees at bottom center, which are outlined and dwarfed by the giant fireball. The hemispherical shock wave is clearly seen by distortion of the cloudy background sky.



**Fig. 6** Large chemical explosion (US Govt. photo by Defense Special Weapons Agency).

In the Fall of 1997, 50 years after an airplane first “broke the sound barrier,” two jet-powered cars vied to accomplish the same feat on the ground. One of them, called *Thrust SSC*, succeeded. Despite



considerable media coverage, only one still image by photographer Chris Rossi managed to capture the attendant shock wave phenomena (Fig. 7). Four oblique shock waves are clearly visible above the vehicle via background distortion of the desert. Less obvious but certainly also present is the bow shock wave, about  $\frac{1}{2}$  vehicle length ahead, normal to the direction of motion, and extending at least as high as the distant background ridgetop. The Mach number of the vehicle in this photo was determined to be 1.02. The observed wave pattern is entirely consistent with that of an artillery projectile at Mach 1.015, as seen in the well-known series of shadowgrams by A. C. Charters[15].



**Fig. 7** Transonic flow about the *Thrust SSC* car. Photo by Chris Rossi, © 1997, reproduced by permission (for more information see <http://www.supersoniccars.com>).

The remaining examples of outdoor schlieren observation are all aviation-related. The shock waves about high-speed aircraft and the exhaust plumes of jet aircraft can become visible by background distortion under proper circumstances. For example, Fig. 8 shows a General Dynamics F-111 fighter in transonic flight at low altitude, with oblique shocks clearly seen against the background light/dark boundary of a mountain ridge. The jet exhaust is also seen. Though similar waves are certainly present above the aircraft, they are not seen against the uniform background of the sky.



**Fig. 8** F-111 fighter (US Govt. photo by Sandia National Laboratories, courtesy D. McBride).

On an expedition for the purpose of photographing shock waves above the wing of an L-1011 commercial jet transport, Fisher et al.[16] captured the image shown in Fig. 9. It is well known that a normal shock wave stands on such an aircraft wing during transonic cruise. Its shadow may be seen by sunlight shadowgraphy (to be discussed later), but the shock itself is almost never visible. Here,

however, the aircraft was banked so as to provide a background of scattered white clouds over the blue Pacific Ocean. By viewing along the shock wave, it is revealed through background distortion.



**Fig. 9** Shock wave on L-1011 wing (US Govt. photo by Carla Thomas, NASA Dryden Research Center).



**Fig. 10** An F-15E Eagle leaps into the air at Mildenhall (UK) Air Fete 1998. Photo by Peter Steehouwer, <http://www.steehouwer.com/>, reproduced by permission.

In Fig. 10 an F-15 fighter jet exhaust shows up by background distortion of the distant trees. The exposure time was short enough to “freeze” turbulence in the exhaust. Note the impression that this exhaust is sharply in focus against a less-distinct background, and the fact that the takeoff rotation



causes the high-speed jet exhaust actually to impinge upon the runway.

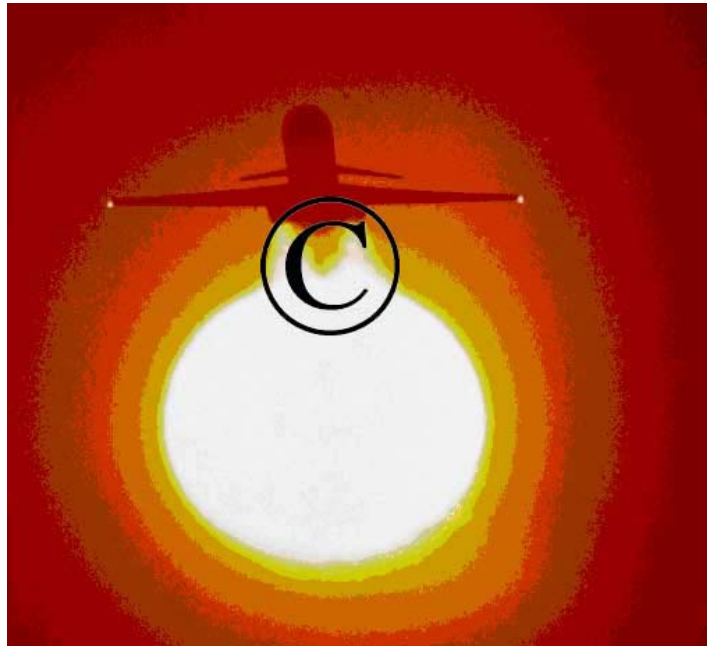


**Fig. 11** A DC-9 takes off against the setting sun. © David Nunuk, Photo Researchers



**Fig. 12** F-4 Phantoms at sunset, Oahu. Photo: Edmund Nägele, F. R. P. S.

Figs. 11 and 12 are two of the best of many photos showing jet aircraft taking off against an enlarged telephoto image of the sun. In such cases the light/dark boundary is very strong and schlieren effects are always visible, revealing the refraction of the jet exhaust. In Fig. 12, by direct inspection, one can see that the refraction angle was about  $1/3$  of the apparent angle subtended by the sun, or about  $1/6^\circ$ . These striking images are very popular in travel advertisements, where they suggest taking off into a serene sunset for places unknown. They never suggest the reality of losing a nights sleep in a crowded metal cylinder!

## SUNLIGHT SHADOWGRAPHY

One may speculate (Fig. 13) that even our prehistoric ancestors had many occasions to see sunlight shadowgrams. The effect is commonplace, requiring only bright sunlight, a strong refractive disturbance in the air, and a relatively-plain surface upon which the shadow is cast. Modern examples include hot plumes from chimneys, expanding spherical shock envelopes from ground-level explosions[3], and a variety of cases arising from aviation.



**Fig. 13** A possible prehistoric sunlight shadowgraphy observation (sketch by author).

A famous example of sunlight shadowgraphy is seen in the original Soviet film of the liftoff of Yuri Gagarin – the first man in space – on April 12, 1961. As Gagarin’s giant Vostok 1 rocket lifted off in the morning sunlight, its shadow was clearly cast on the nearby flat Baikonur terrain. In the wake of the flared rocket, its enormous plume of hot exhaust gases was made visible by sunlight shadowgraphy (Fig. 14).

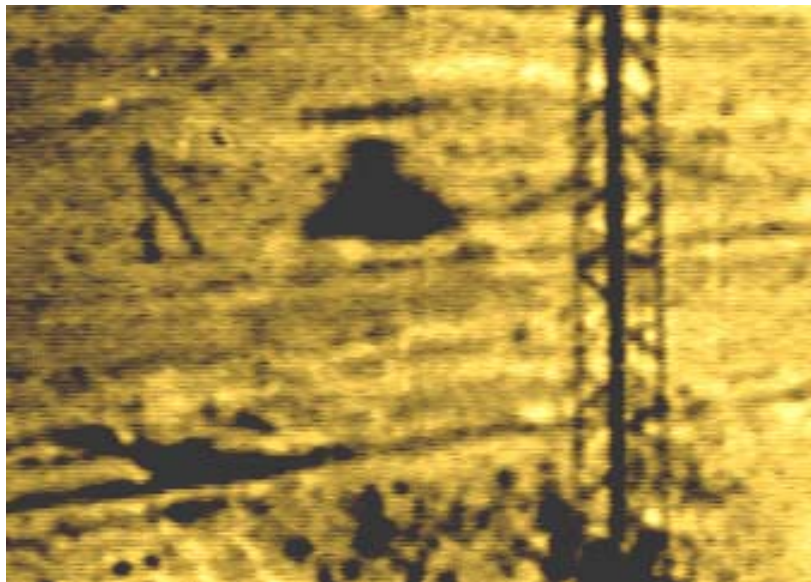


**Fig. 14** Sunlight shadowgram of Gagarin’s historic liftoff (from Soviet footage).

As noted in the introduction, Cooper and Rathert[10] first studied the use of sunlight shadowgraphy to reveal shock wave locations on high-speed aircraft wings. The topic was later addressed by

Crowder[17], and most recently by Fisher et al.[16]. A photograph from the latter study is given in Fig. 15. The effect often may be seen in commercial jet travel when the sun is in the correct position. The wing shock lies spanwise along the wing and roughly normal to it, which means that it is inclined rearward from the vertical by a few degrees. Best shadowgraphy occurs, of course, when the sunlight is approximately tangent to the shock wave. Thus, when the sun is more-or-less overhead or slightly aft thereof, while flying at transonic cruise, look for the sunlight shadowgram of the shock wave on the wing. From experience, not even the flight crew know what causes it.

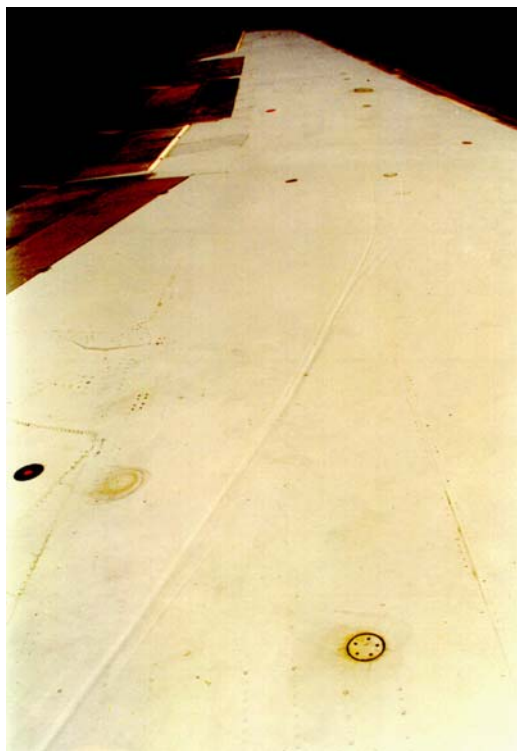


**Fig. 15** Sunlight shadowgram of shock wave on L-1011 wing at transonic cruise (US Govt. photo by Carla Thomas, NASA Dryden Research Center).

### **SPECIAL APPARATUS FOR OUTDOOR IMAGING**

Up to now, all the outdoor observations of refractive disturbances discussed here have been those that are naturally visible to the unaided eye. However, a few enterprising investigators have devised instruments to aid and extend this process. Chief among these is Leonard Weinstein, whose “Schlieren for Aircraft in Flight”[18-23] combined the sun, a telescope, and an appropriate cutoff to produce the most original schlieren instrument in 50 years. His image of a T-38 jet at Mach 1.1 (Fig. 16) set a new standard for the field-of-view of a schlieren instrument, namely more than 80m in width.

Weinstein’s second achievement in outdoor schlieren imaging[19, 22, 24] was the combination of a fixed vertical light source, matching cutoff, and streak camera that produced, for the first time, schlieren images of rocket sled testing of a quality comparable to images obtained indoors in the laboratory. An excellent example is shown in Fig. 17. This approach suggests a related possibility of imaging outdoor schlieren objects using a portable scanning light source (e.g. a moving fluorescent bulb), a synchronized scanning cutoff, and a time-delay-integration camera.

Other examples of outdoor apparatus include a parallel-beam schlieren setup of 8m length for atmospheric turbulence observations[25] and a submersible shadowgraph built for the purpose of studying interface behavior in salt-gradient solar ponds[26]. Edgerton[27] took outdoor shadowgrams of explosions using a strobe lamp and a unique black retroreflective screen. Winn and Morin[28] used a convex automotive rear-view mirror to reduce the sun’s apparent size for sunlight shadowgrams cast on a projection screen in an open, darkened garage. Sharp shadowgrams of gasoline vapors and their



ignition were obtained. Likewise the glint from sunlight reflecting off convex glass or chrome outdoors is sometimes projected indoors through a window, casting a sharp shadow. Finally, Dalziel et al.[29] used real-time image processing electronics to subtract the background from imagery of foreground schlieren objects. This “synthetic schlieren” approach might be used outdoors at large scale, given backgrounds such as that shown in Fig. 4.

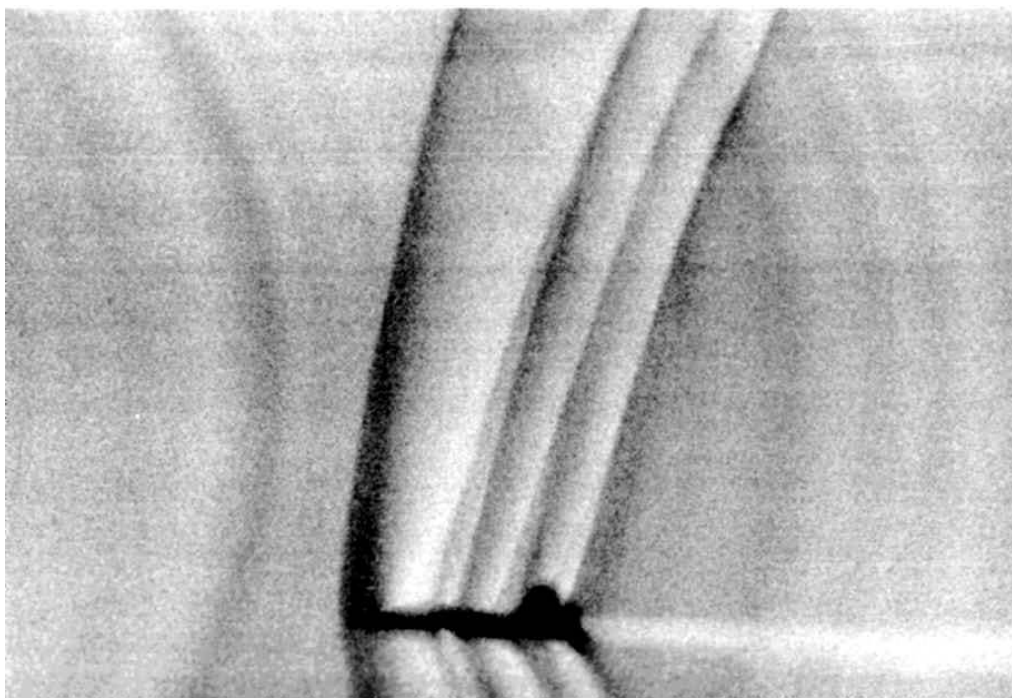


**Fig. 16** T-38 at Mach 1.1, Schlieren for aircraft in flight (US Govt. photo by Leonard M. Weinstein, NASA Langley Research Center).

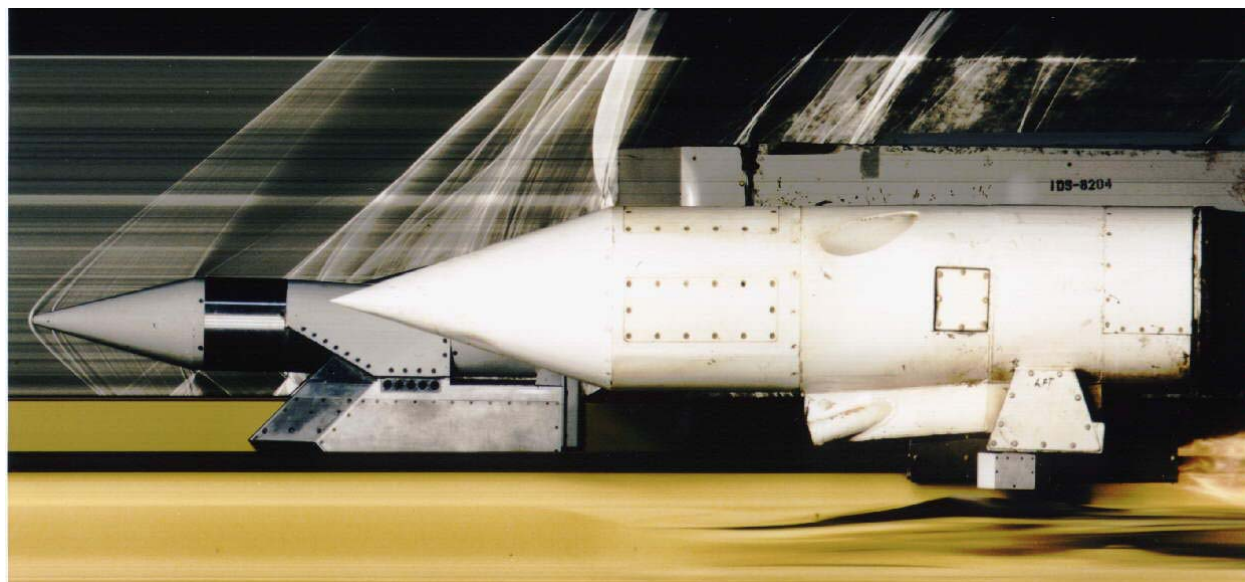


**Fig. 17** Holloman AFB high-speed test track Maglev model, Mach 1.8, Ref.[24] (US Govt. photo courtesy Leonard M. Weinstein).

## CONCLUSION

A general review has been given of outdoor schlieren and shadowgraphy. Optical principles were first discussed for the two main approaches: sunlight shadowgraphy and schlieren by background distortion. Examples were then cited and illustrations shown for a variety of outdoor observations of thermal convection, combustion, and shock wave phenomena. While some of these amount to no more than curiosities, others are significant in providing important and useful flow visualizations. There is untapped potential here as well: gas leak detection, thermal studies of large outdoor equipment, aerodynamics of ground transportation, and even meteorological visualizations on a grand scale are possible in principle.

Schardin [8, 9] concluded: "Although coarse schlieren can be seen with the naked eye, the construction of special apparatus is necessary for more accurate observation..." This remains true today; outdoor observations of schlieren and shadowgraphy do not replace the more familiar laboratory instruments. However, they do give us unique insight into outdoor processes under circumstances and at scales that are impossible to duplicate in the laboratory.

## ACKNOWLEDGEMENTS

I gratefully acknowledge the assistance of Dr. Leonard Weinstein (NASA), the support of J. D. Miller and Lori J. Dodson-Dreibelbis (Penn State Gas Dynamics Lab), and the encouragement of Dr. Peter Krehl (Ernst-Mach-Institut). The several individuals and organizations who contributed valuable images are named in the figure captions, and are thanked for their assistance.

## REFERENCES

1. Hooke, R., *Micrographia*, J. Martyn & J. Allestry, London, 1665.
2. Rienitz, J., Schlieren Experiment 300 Years Ago, *Nature*, Vol. 254, No. 5498, pp. 293-295, 1975.
3. Mach, E., On some phenomena attending the flight of projectiles, *Popular Scientific Lectures*, ed. McCormack, T.J., Open Court Pub. Co., La Salle, IL, pp. 309-337, 1943.
4. Melsens, M., Sur les plaies produits par les armes a feu, *Soc. Royale d. Sciences Medicales*, Brussels, 1872.
5. Riemann, G. F. B., Über die Fortpflanzung ebener Luftwellen von endlicher Swingungsweite, *Abhandlung d.Göttingen Gesellschaft d.Wissenschaft*, Vol. 8, pp. 43-1860.
6. Mach, E. and Salcher, P., Photographische Fixirung der durch Projectile in der Luft eingeleiteten Vorgänge, *Sitzungsberichte der kaiserliche Academie der Wissenschaften, Mathematik-Naturwissenschaftliche Klasse, Wien*, Vol. 95, pp. 764-786, 1887.
7. Douglass, A. E., Atmosphere, Telescope, and Observer, *Amateur Telescope Making*, ed. Ingalls, A.G., Scientific American, New York, pp. 585-605, 1980.
8. Schardin, H., Die Schlierenverfahren und ihre Anwendungen, *Ergebnisse der Exakten Naturwissenschaften*, Vol. 20, pp. 303-439, 1942.
9. Schardin, H., Schlieren methods and their applications, *Report TT-F-12731*, NASA, Washington, DC, 1970.
10. Cooper, G.E. and Rathert, G.A., Visual observations of the shock wave in flight, *Report RM A8C25*, NACA, 1948.
11. Dvorák, V., Über eine neue einfache Art der Schlierenbeobachtung, *Wiedemanns Annalen der Physik und Chemie*, Vol. 9, No. 3, pp. 502-511, 1880.
12. Marat, J.P., *Recherches physiques sur le feu*, Cl. Ant. Jombert, Paris, France, 1780.
13. Rienitz, J., Optical inhomogeneities: schlieren and shadowgraph methods in the seventeenth and eighteenth centuries, *Endeavor*, Vol. 21, No. 2, pp. 77-81, 1997.
14. Holder, D.W. and North, R. J., *Schlieren methods*, NPL Notes on Applied Science No. 31, Her Majesty's Stationery Office, London, 1963.
15. Van Dyke, M., *An album of fluid motion*, Parabolic Press, PO Box 3032, Stanford, CA, 1982.
16. Fisher, D.F., Haering, E.A., Jr., Noffz, G.K., and Aguilar, J.I., Determination of sun angles for observations of shock waves on a transport aircraft, *Report TM-1998-206551*, NASA, 1998.

17. Crowder, J. P., Flow visualization techniques applied to full-scale vehicles, *AIAA Atmospheric Flight Mechanics Conference, Monterey, CA, Aug. 17-19, 1987*, AIAA, NY, pp. 164-171, 1987.
18. Weinstein, L. M., An Optical Technique for Examining Aircraft Shock Wave Structures in Flight , *High-Speed Research: 1994 Sonic Boom Workshop*, NASA CP 3279, pp. 1-17, 1994.
19. Weinstein, L. M., Schlieren system and method for moving objects, US Patent 5,534,995, Feb., 1995.
20. Weinstein, L. M., An Electronic Schlieren Camera for Aircraft Shock Wave Visualization, *NASA High-Speed Research Program Sonic Boom Workshop, 1995*, Vol. 1, pp. 244-258, 1996.
21. Weinstein, L. M., Stacy, K., Vieira, G. J., Haering, E. A., Jr., and Bowers, A. H., Visualization and image processing of aircraft shock wave structures, *1st Pacific Symposium on Flow Visualization and Image Processing, Feb. 23-26, 1997, Honolulu, Hawaii, 1997*.
22. Weinstein, L. M., Large field schlieren visualization - from wind tunnels to flight, *Intl. Conf. on Optical Technology and Image Processing in Fluid, Thermal, and Combustion Flow, Yokohama, Japan, VSJ-SPIE98*, Paper AB124, Dec. 1998.
23. Weinstein, L. M., Culliton, W., and Rivers, R., Visualization of transonic flow over a T-38 aircraft, *Proceedings of the 8th International Symposium on Flow Visualization, Sorrento, Italy, 1998*.
24. Weinstein, L. M. and Minto, D., Focusing Schlieren Photography at the Holloman High Speed Test Track, *Proc. of the 22nd International Congress on High-Speed Photography and Photonics, Santa Fe, NM, Vol. 2869, SPIE , Bellingham, WA, pp. 865-873, 1996*.
25. Eaton, F. D., Peterson, W. A., Hines, J. R., Drexler, J. J., Soules, D. B., Waldie, A. H., and Qualtrough, J. A., Morphology of atmospheric transparent inhomogeneities, *Propagation engineering: 3<sup>rd</sup> in a series; Proceedings of the Meeting, Orlando, FL, Vol. 1312, SPIE, Bellingham, WA, pp. 134-146, 1990*.
26. Huacuz, J. M., Sierra, F., Venegas, C., and Ramos, C., Construction and test of a submersible shadowgraph for in-pond study of interface behavior, *Solar Engineering 1989 - Proceedings of the Eleventh Annual ASME Solar Energy Conference*, ASME, New York, pp. 407-412, 1989.
27. Edgerton, H.E., *Electronic Flash, Strobe*, edition 3, MIT Press, Cambridge, MA, 1970.
28. Winn, R. C. and Morin, C. R., Low cost shadowgraph technique for flammable vapor visualization, *IECEC-97; Proceedings of the 32nd Intersociety Energy Conversion Engineering Conference, Honolulu, HI, Vol. 1, American Institute of Chemical Engineers, NY, pp. 642-647, 1997*.
29. Dalziel, S. B., Hughes, G. O., and Sutherland, B. R., Synthetic Schlieren, *Proceedings of the 8<sup>th</sup> International Symposium on Flow Visualization, Sorrento, Italy, Paper No. 62, 1998*.